

# Control of Intramolecular Orbital Alignment in the Photodissociation of Thiophenol: Conformational Manipulation by Chemical Substitution\*\*

Jeong Sik Lim, Yoon Sup Lee, and Sang Kyu Kim\*

As scientists understand chemical reactions in atomic detail, many successful examples of reaction control have been reported in recent decades. These include active control using pulse shaping in terms of chirps or phases<sup>[1–5,20]</sup> or passive control, such as vibration-mediated photodissociation.<sup>[6–13]</sup> Apart from these studies, an interesting structure-based approach relying on conformational specificity has recently been introduced as an alternative tool for reaction control. In this approach, a particular conformational isomer is exclusively chosen, and its unique chemical reactivity is thoroughly examined. For instance, in the photodissociation of the cation of 1-iodopropane, a *gauche* or *trans* conformational isomer was selectively prepared by the mass-analyzed threshold ionization (MATI) technique, and it was found that different conformational isomers give rise to totally different reaction products.<sup>[14]</sup> Another example of conformer-specific reaction control has been demonstrated by Suits and co-workers in the photodissociation of the *gauche* or *cis* conformational isomers of the cation of 1-propanal. In the latter case, one of two reaction channels proceeding in the ground state is preferentially controlled by conformational selection in the excited state.<sup>[15]</sup> More recently, alanine and  $\beta$ -alanine, which are biological building blocks, were also found to be quite conformer-specific in their decarboxylation reactions upon ionization.<sup>[16]</sup> The relationship between structure and chemical reactivity is essential for the understanding and control of chemical reactions, and therefore the study of the conformational specificity at the atomic level seems to be invaluable at the present time.

Herein, we use the conformational change upon chemical substitution to control the branching ratio of two reaction channels in the photodissociation of thiophenol and its derivatives. It has been found that, as a result of S–H(D) dissociation, the phenylthiyl radical is produced with its reactive singly occupied molecular orbital (SOMO) either perpendicular ( $\tilde{X}$ ) or parallel ( $\tilde{A}$ ) to the molecular plane.<sup>[17]</sup> This so-called “intramolecular orbital alignment” is a novel concept in stereodynamics that could be developed into a

useful tool in stereochemistry. Accordingly, control of the branching ratio naturally means that the intramolecular orbital alignment in the reactive phenylthiyl radical could be controlled by manipulation of the photodissociation dynamics.

[D]Thiophenol ( $C_6H_5SD$ ) is excited to the  $S_2$  state via the  $^1(n,\sigma^*)$  transition at a pump energy of 243 nm, with subsequent prompt S–D dissociation, the time scale of which is less than 100 fs.<sup>[18]</sup> Since the repulsive  $S_2$  state belongs to  $A''$  whereas the ground  $S_0$  state belongs to  $A'$ , the diabatic potential-energy surfaces of  $S_2$  and  $S_0$  cross along the S–D elongation coordinate, as  $S_2$  and  $S_0$  diabatically correlate to the  $\tilde{X}$  and  $\tilde{A}$  states of phenylthiyl ( $C_6H_5S$ ), respectively.<sup>[18]</sup> This dissociation may be qualitatively described as the dynamics of a simple wavepacket on potential-energy surfaces (PES) of reduced dimensionality. In this picture, the bifurcation of the wavepacket into two different  $\tilde{A}$  and  $\tilde{X}$  states of phenylthiyl takes place at the conical intersection (CI), which is formed at the planar geometry for which the plane of symmetry is maintained along the reaction coordinate (Figure 1).

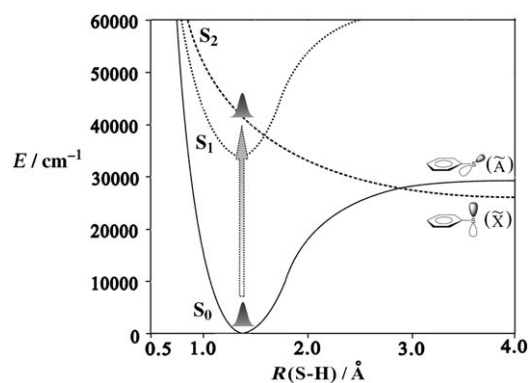


**Figure 1.** Diabatic potential-energy surfaces of thiophenol along the S–H bond elongation coordinate at planar geometry. At 243 nm, the wavepacket is exclusively prepared on  $S_2$ .

In recent theoretical studies on the photodissociation dynamics of phenol, the out-of-plane torsional motion of OH with respect to the benzene moiety is found to be the most critical mode in the bifurcation dynamics at the conical intersection.<sup>[19,20]</sup> The PES of thiophenol involved in optical excitation and bond dissociation are intrinsically very similar to those of phenol, except for detailed shapes and energetics, especially at the asymptotic limit (Figure 1). Therefore, the

[\*] J. S. Lim, Prof. Y. S. Lee, Prof. S. K. Kim  
Department of Chemistry and School of Molecular Science (BK21)  
Korea Advanced Institute of Science and Technology (KAIST)  
Daejeon 305-701 (Republic of Korea)  
Fax: (+82)-42-869-2810  
E-mail: sangkyukim@kaist.ac.kr

[\*\*] We would like to acknowledge the support from KOSEF (R01-2007-000-10766-0, R11-2007-012-01002-0), Echotechnopia 21 project of KIEST (102-071-606), and KISTI Supercomputing Center (KSC-2007-S00-1027).

theoretical result obtained for phenol can naturally be adopted to explain the bifurcation dynamics on the CI in thiophenol dissociation. Namely, if the initial wavepacket position on the potential-energy surface along the C-C-S-D angle can be chosen arbitrarily, then dynamics on the CI may be manipulated to give the control over two different reaction channels, in this case the  $\tilde{X}$  and  $\tilde{A}$  states of phenylthiyl. It is noteworthy that optimal control as an alternative approach has been theoretically simulated for the photodissociation of phenol.<sup>[20]</sup> At the 243-nm excitation of thiophenol and its derivatives, the wavepacket is prepared on the repulsive  $S_2$  state with subsequent diabatic passage through the  $S_2/S_1$  conical intersection. The  $\tilde{X}/\tilde{A}$  state bifurcation takes place at the  $S_2/S_0$  CI, whereas the total yield might depend on the  $S_2/S_1$  crossing dynamics.

[D]Thiophenol in the ground state has a planar geometry in which the SD moiety lies in the plane of symmetry. When the molecule is excited to the  $S_2$  state, the potential-energy surface is repulsive in nature along the S–D elongation axis. However, the potential-energy surface becomes more strongly bound along the C-C-S-D angle in the  $S_2$  state than in  $S_0$ , according to our time-dependent density functional theory (TDDFT) calculations (Figure 2).<sup>[21]</sup> The minimum-energy geometry remains at  $0^\circ$  in the  $S_2$  state, where  $0^\circ$  is defined as the C-C-S-D dihedral angle at the planar geometry. Therefore, according to the Franck–Condon principle, the wavepacket is initially prepared at the bottom of the valley in

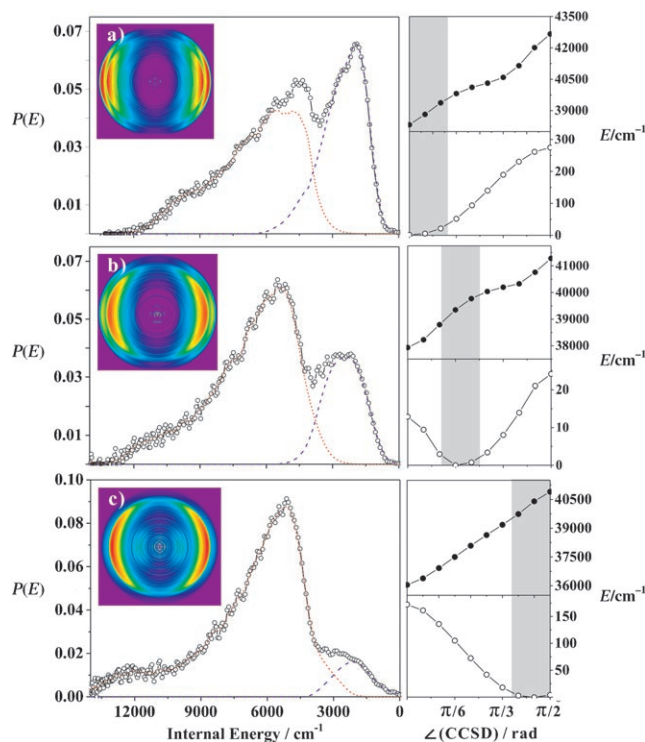


**Figure 2.** Internal energy distributions ( $\circ$ ) of  $\text{XC}_6\text{H}_4\text{S}$  and the deconvoluted  $\tilde{X}$  (---) and  $\tilde{A}$  states (---) deduced from corresponding D images taken at 243 nm for a)  $\text{X}=\text{H}$ , b)  $\text{X}=\text{F}$ , and c)  $\text{X}=\text{OCH}_3$ . On the right, potential-energy curves along the C-C-S-D dihedral angle are shown for the ground ( $\circ$ ) and  $S_2$  ( $\bullet$ ) states. Franck–Condon regions are shaded.

two-dimensional PES with respect to the C-C-S-D dihedral angle. As the wavepacket moves on the repulsive surface, it spreads out along the S–D bond elongation axis, but it remains localized around the  $0^\circ$  geometry, since little torque is exerted on the torsional angle in such an ultrafast wavepacket motion, as depicted in Figure 3. Since the CI exists at the

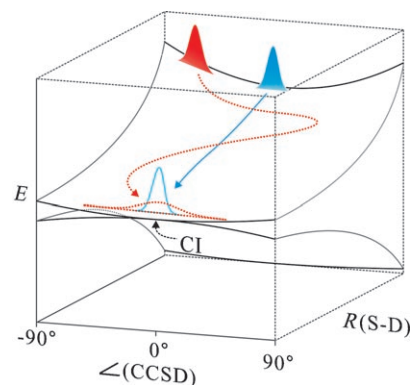




**Figure 3.** A simple wavepacket propagation model on two-dimensional PES. The  $S_2/S_0$  conical intersection is formed at the planar geometry. As the initial location of the optically prepared wavepacket is changed, the bifurcation dynamics on the CI are expected to be strongly dependent on the two-dimensional wavepacket spreads.

planar geometry, the diabatic passage of the wavepacket through the CI is expected to be significant. Experimental findings are consistent with this prediction. Namely, as reported earlier, the yield of the  $\tilde{X}$  state resulting from the diabatic passage through the CI is measured to be 0.43, whereas that of the  $\tilde{A}$  state is 0.57 in the photodissociation of thiophenol at 243 nm.<sup>[18]</sup> Even though vibrational modes other than C-C-S-D torsion and S–D stretching may also affect dissociation dynamics in general, the bifurcation dynamics in the vicinity of the CI are not expected to be significantly influenced by those, as pointed out by Domcke and co-workers.<sup>[19]</sup>

For the control, we can then imagine that the manipulation of the initial location of the wavepacket on 2D PES as the change of the initial location of the wavepacket along the C-C-S-D angle should result in different bifurcation dynamics at the CI. In this case, we have utilized the fact that the C-C-S-D dihedral angle in the ground state is changed as the chemical group at the *para* position of thiophenol is substituted. It has been reported that when an electron-donating group is substituted at the *para* position, the SH moiety of thiophenol becomes nonplanar in the ground state.<sup>[22]</sup> For instance, for [D]4-methoxythiophenol, in which the *para* position is substituted with the methoxy ( $\text{OCH}_3$ ) group, the C-C-S-D dihedral angle becomes  $73^\circ$ , according to our DFT calculations<sup>[21]</sup> and reference [22]. This finding means that the SD moiety becomes almost perpendicular to the molecular plane in the ground state of 4-methoxythiophenol. In the  $S_2$  state, however, the minimum-energy structure adopts the planar geometry. This result suggests that the overall shape of the upper PES remains same as that of thiophenol, whereas the initial location of the wavepacket is changed to the edge

near the top of the downhill potential along the C-C-S-D angle for [D]4-methoxythiophenol (Figure 2). Accordingly, there will be a strong torque exerted on the C-C-S-D dihedral angle as the wavepacket moves out along the repulsive S-D coordinate. Therefore, as the reaction proceeds, the wavepacket will be spread out not only along the S-D bond axis but also along the C-C-S-D angle. The wide spread of the wavepacket at the  $S_2/S_0$  conical intersection is expected to diminish the probability of the diabatic passage through the CI significantly. Consistently, the experiment shows a dramatic decrease of the  $\tilde{X}$  state population, giving a yield of 0.09 for  $\tilde{X}$  (0.91 for  $\tilde{A}$ ) in the photodissociation of 4-methoxythiophenol (Figure 2 and Table 1). In other words, the reaction follows the adiabatic surface with a 91% probability, whereas the diabatic passage through the CI occurs with a probability of only 9%.

**Table 1:** Yields of the  $XC_6H_4S$  ( $X = H, F, OCH_3$ ) radical.

$\tilde{X}$ (CCSD)	0° ( $X = H$ )	31° ( $X = F$ )	73° ( $X = OCH_3$ )
	57%	74%	91%
	43%	26%	9%

Further exploration has been carried out for 4-fluorothiophenol. According to the TDDFT calculations, the most stable structure of [D]4-fluorothiophenol adopts a geometry in which the C-C-S-D angle is 31° in the ground state, whereas it has the minimum energy at the planar geometry in the  $S_2$  state (Figure 2). In this case, the initial wavepacket will be located on the middle of the downhill potential along the C-C-S-D angle. Therefore, the diabatic passage through the CI will be less significant than for thiophenol but more probable than for 4-methoxythiophenol, because the extent of the wavepacket spread along the dihedral angle in the vicinity of the CI is likely to be between those of the two other cases. Experimental findings support this simple model, giving 0.26 and 0.74 for yields of the  $\tilde{X}$  and  $\tilde{A}$  states, respectively, for 4-fluorothiophenol (Table 1). It should be noted that the  $\tilde{X}$ - $\tilde{A}$  energy gaps of phenylthiyl derivatives ( $XC_6H_4SD$ ;  $X = H, CH_3O, F$ ) are found to be almost identical, thus indicating that the relative energy of the SOMO localized on sulfur (3p) is only slightly affected by the chemical substitution. The S-D bond energy is slightly affected by the chemical substitution. The UV absorption spectra of all thiophenol derivatives studied herein show very similar features at around 243 nm, where the  $S_2 \leftarrow S_0$  transition is dominant.

Another way of manipulating the wavepacket location on  $S_2$  would be the selective excitation of the out-of-plane C-C-S-D torsional mode in the ground state. However, such an IR-UV double excitation scheme is experimentally quite demanding, as the actual torsional mode frequency is too low (less than  $100 \text{ cm}^{-1}$ ) to be excited by a conventional IR laser pulse. In this case, the backing pressure of the supersonic jet is varied to change the vibrational temperature of the

sample to possibly excite low-frequency modes. In Figure 4, the translational energy distributions from the photodissociation of [D]4-fluorothiophenol at 243 nm are compared for

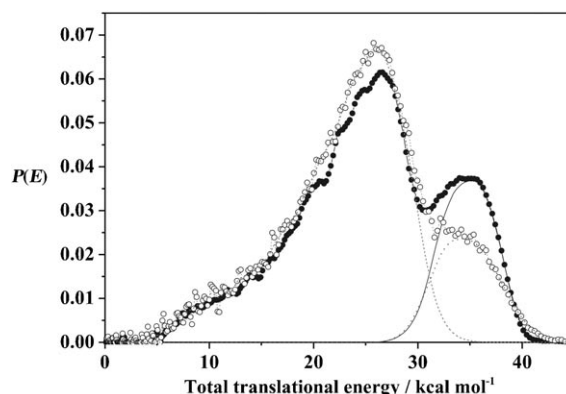


**Figure 4.** Total translational energy distribution from the photodissociation of [D]4-fluorothiophenol at a backing pressure of 3 atm (●) and 0.5 atm (○). The distributions are normalized for the comparison. A long tail at the high translational energy region in the distribution at 0.5 atm indicates that the molecule in the jet is vibrationally hot.

two different jet conditions. As the helium backing pressure goes down from 3 atm to 0.5 atm, the temperature of the jet increases because of the increase of the seeding ratio. The DFT torsional frequency of 4-fluorothiophenol is  $29 \text{ cm}^{-1}$ ,<sup>[23]</sup> and it is most likely that a significant portion of the molecules in the warm jet populate the vibrationally excited state with several quanta of the C-C-S-D torsional mode. Since the torsional barrier height is calculated to be very low in the ground state for 4-fluorothiophenol (Figure 2), the UV excitation of the molecule in the warm jet would result in the widening of the initial wavepacket location in the two-dimensional potential-energy surface along the C-C-S-D dihedral angle. Therefore, the wavepacket will experience more significant spread at the CI, giving the lower probability of diabatic passage to the  $\tilde{X}$  state of the fragment. Quite consistently, the experiment gives a yield of 0.18 for the  $\tilde{X}$  state of  $FC_6H_4S$  in the warm jet, which is much less than the  $\tilde{X}$  yield of 0.26 measured for the molecule in the cold jet. This experimental finding strongly supports the above two-dimensional bifurcation dynamics at the CI.

In conclusion, we have employed the conformational preference of thiophenol derivatives to manipulate the initial location of the wavepacket along the C-C-S-D dihedral-angle coordinate on two-dimensional PES leading to prompt S-D bond dissociation. The branching ratio between  $\tilde{X}$  and  $\tilde{A}$  states of the final fragment is controlled by the conformational preference induced by chemical substitution at the *para* position of [D]thiophenol. The experimental trend is successfully explained by the simple wavepacket propagation model. Namely, the wavepacket spread along the C-C-S-D dihedral angle either through conformational control or vibrational excitation strongly affects the probability of diabatic passage through the conical intersection in such a way that the probability of the diabatic passage at the CI diminishes as the

wavepacket gets spread out along the C-C-S-D angle. The control of the branching ratio of between  $\tilde{X}$  and  $\tilde{A}$  states has a special meaning in the case of the phenylthiyl radical, since it is now possible to control the intramolecular orbital alignment. Further investigation of bimolecular reactions under the control of the intramolecular orbital alignment would be quite meaningful in the field of stereochemistry. Theoretical wavepacket dynamics studies on ab initio two-dimensional PES for thiophenol and its derivatives are highly desirable in near future.

## Experimental Section

Detailed experimental conditions have been described elsewhere.<sup>[18,24]</sup> Briefly, all samples were heated to 60°C, mixed with the He carrier gas, and expanded into vacuum. The D images were taken for all velocity components and averaged over 36000 laser shots. The three-dimensional images were reconstructed from raw images using the LV-pBASEX<sup>[25]</sup> or BASEX<sup>[26]</sup> algorithm. Total translational energy distributions were corrected by the Jacobian factor.

Received: November 22, 2007

**Keywords:** conformational isomerism · conical intersections · photodissociation · reaction mechanisms

- [1] a) A. Dantus, *Annu. Rev. Phys. Chem.* **2001**, *52*, 639–679; b) I. Pastirk, J. Brown, Q. Zhang, M. Dantus, *J. Chem. Phys.* **1998**, *108*, 4375–4378.
- [2] R. J. Gordon, S. A. Rice, *Annu. Rev. Phys. Chem.* **1997**, *48*, 601–641.
- [3] a) A. Assion, T. Baumert, M. Bergt, T. Brixner, B. Kiefer, V. Seyfried, M. Strehle, G. Gerber, *Science* **1998**, *282*, 919–922; b) T. Brixner, N. H. Damrauer, P. Niklaus, G. Gerber, *Nature* **2001**, *414*, 57–58; c) A. Assion, T. Baumert, J. Helbing, V. Seyfried, G. Gerber, *Chem. Phys. Lett.* **1996**, *259*, 488–494.
- [4] a) L. Zhu, V. Kleiman, X. Li, S. P. Lu, K. Trentelman, R. J. Gordon, *Science* **1995**, *270*, 77–79; b) L. Zhu, K. Suto, J. A. Fiss, R. Wada, T. Seidman, R. J. Gordon, *Phys. Rev. Lett.* **1997**, *79*, 4108–4111.
- [5] a) C. J. Bardeen, V. V. Yakovlev, K. R. Wilson, S. D. Carpenter, P. M. Weber, W. S. Warren, *Chem. Phys. Lett.* **1997**, *280*, 151–158; b) V. V. Yakovlev, C. J. Bardeen, J. W. Che, J. S. Cao, K. R. Wilson, *J. Chem. Phys.* **1998**, *108*, 2309–2313.
- [6] a) F. F. Crim, *Annu. Rev. Phys. Chem.* **1993**, *44*, 397–428; b) M. D. Likar, J. E. Baggott, A. Sinha, T. M. Ticich, R. L. Vander Wal, F. F. Crim, *J. Chem. Soc. Faraday Trans. 2* **1988**, *84*, 1483–1497.
- [7] a) A. Sinha, M. C. Hsiao, F. F. Crim, *J. Chem. Phys.* **1990**, *94*, 4928–4935; b) A. Sinha, M. C. Hsiao, F. F. Crim, *J. Chem. Phys.* **1990**, *92*, 6333–6335; c) R. L. Vander Wal, J. L. Scott, F. F. Crim, *J. Chem. Phys.* **1990**, *92*, 803–805.
- [8] a) R. L. Vander Wal, F. F. Crim, *J. Phys. Chem.* **1989**, *93*, 5331–5333; b) R. Schinke, R. L. Vander Wal, J. L. Scott, F. F. Crim, *J. Chem. Phys.* **1991**, *94*, 283–289.
- [9] a) T. M. Ticich, M. D. Likar, H. R. Dübal, L. J. Butler, F. F. Crim, *J. Chem. Phys.* **1987**, *87*, 5820–5829; b) M. Brouard, M. T. Martinez, J. O'Mahony, J. P. Simons, *J. Chem. Soc. Faraday Trans. 2* **1989**, *85*, 1207–1219.
- [10] A. Sinha, R. L. Vander Wal, F. F. Crim, *J. Chem. Phys.* **1989**, *91*, 2929–2938.
- [11] a) S. S. Brown, R. B. Metz, H. L. Berghout, F. F. Crim, *J. Chem. Phys.* **1996**, *105*, 6293–6303; b) H. L. Berghout, S. S. Brown, R. Delgado, F. F. Crim, *J. Chem. Phys.* **1998**, *109*, 2257–2263.
- [12] a) A. Bach, J. M. Hutchison, R. J. Holiday, F. F. Crim, *J. Phys. Chem. A* **2003**, *107*, 10490–10496; b) A. Bach, J. M. Hutchison, R. J. Holiday, F. F. Crim, *J. Chem. Phys.* **2002**, *116*, 4955–4961.
- [13] S. M. Holland, R. J. Stickland, M. N. R. Ashfold, D. A. Newnham, I. M. Mills, *J. Chem. Soc. Faraday Trans.* **1991**, *87*, 3461–3471.
- [14] S. T. Park, S. K. Kim, M. S. Kim, *Nature* **2002**, *415*, 306–308.
- [15] M. H. Kim, L. Shen, H. Tao, T. J. Martinez, A. G. Suits, *Science* **2007**, *315*, 1561–1565.
- [16] K. W. Choi, D. S. Ahn, J. H. Lee, S. K. Kim, *Chem. Commun.* **2007**, 1041–1043.
- [17] J. S. Lim, I. S. Lim, K. S. Lee, D. S. Ahn, Y. S. Lee, S. K. Kim, *Angew. Chem.* **2006**, *118*, 6438; *Angew. Chem. Int. Ed.* **2006**, *45*, 6290.
- [18] I. S. Lim, J. S. Lim, Y. S. Lee, S. K. Kim, *J. Chem. Phys.* **2007**, *126*, 034306.
- [19] Z. Lan, W. Domcke, V. Vallet, A. L. Sobolewski, S. Mahapatra, *J. Chem. Phys.* **2005**, *122*, 224315.
- [20] M. Abe, Y. Ohtsuki, Y. Fujimura, Z. Lan, W. Domcke, *J. Chem. Phys.* **2006**, *124*, 224316.
- [21] Gaussian 03 package was used for constructing PES. The potential of  $S_0$  was constructed by full optimization, except the C-C-S-D dihedral angle and S–H distance, at the B3LYP/6-311++G(d,p) level. The torsional PES was obtained by calculating  $S_2$  vertical excitation energies with the time-dependent DFT method (B3LYP/6-311++G(d,p)).
- [22] P. Mulder, O. Mozenon, S. Lin, C. E. S. Bernardes, M. E. Minas da Piedade, A. F. L. O. M. Santos, M. A. V. Ribeiro da Silva, G. A. Dilabio, H. G. Korth, K. U. Ingold, *J. Phys. Chem. A* **2006**, *110*, 9949–9958.
- [23] Vibration frequencies of 4-fluorothiophenol-d<sub>4</sub> are calculated at the B3LYP/6-311++G(d,p) level considering the deuterium exchange.
- [24] K. S. Lee, J. S. Lim, D. S. Ahn, K. W. Choi, S. K. Kim, *J. Chem. Phys.* **2006**, *124*, 124307.
- [25] a) G. A. Garcia, L. Nahon, I. Powis, *Rev. Sci. Instrum.* **2004**, *75*, 4989–4996; b) special thanks go to Dr. Lionel Poisson (lionel.poisson@cea.fr) for offering the LABVIEW-based pBASEX code.
- [26] V. Dribinski, A. Ossadtchi, V. A. Mandelshtam, H. Reisler, *Rev. Sci. Instrum.* **2002**, *73*, 2634–2642.